Facile assembly of polyoxometalate-polyelectrolyte films on nano-MO_2 (M = Sn, Ti) for optical applications

Sara Usai[a,b] and James J. Walsh[a,b]*

a. School of Chemical Sciences, Dublin City University, Glasnevin, Dublin 9, Ireland.
b. National Centre for Sensor Research, Dublin City University, Glasnevin, Dublin 9, Ireland.

* To whom correspondence should be addressed. Email: james.walsh@dcu.ie

Keywords: polyoxometalate, self-assembly, nanoparticle, electrochromism, polycation, metal oxide.

Abstract

The polyoxometalate $[PMo_{12}O_{40}]^{3-}$ (POM) has been deposited onto high surface area nano-SnO_2 using a polycation. The POM surface coverage recorded was approximately 17 times higher than that achieved on planar substrates using the same method, reducing considerably the time needed to assemble conducting films suitable for optical applications such as electrochromism. The immobilisation of the analogous tungstate $[PW_{12}O_{40}]^{3-}$ onto a nano-TiO_2 semiconductor electrode demonstrates the versatility of this approach, and underscores potential applications using a large combination of polyoxomolybdates or polyoxotungstates with various metal oxide films.

1. Introduction

Polyoxometalates comprise a wide class of molecular metal oxide clusters suitable for diverse applications spanning photochemistry, electrochemistry, catalysis, and sensing.[1] The majority of POMs are anionic, rendering them highly soluble in either water or organic solvents, depending on the counterion employed. Relatively ordered POM films can be created through layer-by-layer (LBL) assembly consisting of alternating polyelectrolyte and POM layers. This involves alternately dip-coating an electrode material into solutions of anionic POM and various cationic species, rinsing between each cycle, to build up multilayer structures. This method is straightforward, removes the need for complex covalent modification of the POM, is robust, and is widely applicable to a host of POM-based systems.[2]

However, there are several disadvantages to the electrostatic multilayer LBL approach. First, each cycle deposits approximately a monolayer of POM and thick (of the order of 100-200 nm) films require multiple deposition cycles which is a slow process, e.g., a 16-bilayer film requires 32 dip steps and would only be *ca*. 100 nm thick.[3] Second, we have shown previously that the rate of charge transport through thicker films consisting of the polyoxometalate α-$[S_2Mo_{18}O_{62}]^{4-}$ and a polycationic Ru(II) metallopolymer is slow due to mass transfer limitations, making thicker films less useful in photoelectrocatalytic applications (time to electrolyse whole film 2 - 50 s).[4] In principle, low film conductivity can generally be addressed by either (a) increasing the supporting electrolyte concentration or (b) by incorporating conducting materials into the film - this has successfully been used in electrocatalytic applications using, for example, multi-walled carbon nanotubes.[5] However, for applications involving an optical component (photocatalysis, photoelectrochemistry, colorimetric sensing, electrochromic displays, photochromism) the addition of particulate or coloured materials into a film can, while rendering the film conducting, also significantly change its optical properties. In addition, high electrolyte concentrations can disrupt the electrostatic interactions which drive the formation of the film.[6] The ideal POM based film would therefore be facile to assemble, be optically transparent, and be amenable to fast potential switching.

Fluorine-doped tin oxide (FTO) has found widespread use as a transparent, planar conducting substrate in photovoltaics and photoelectrochemistry. However, monolithic, planar materials are a poor choice for catalysis and light harvesting due to their inherently low surface areas. Nanoparticle films immobilised on FTO have been used extensively over the past decades to increase surface loading of the material of interest, in effect making a transparent, high surface area electrode; in particular TiO_2 has been used to great effect in dye-sensitized solar cells.[7] While TiO_2 makes an excellent electrode material for immobilising electrocatalyst molecules, its semiconducting properties render it an insulator at positive potentials when in the dark, and is therefore only useful for materials with redox potentials over a limited potential window. In contrast, nano-SnO_2 is electroactive over the

same potential window as FTO and thus suitable for accessing a wide range of redox potentials. In recent years, these outstanding electrical and optical qualities have led several groups working in solar fuels research to utilise nano-SnO_2 to immobilise molecular catalysts for both water splitting half reactions.[8, 9]

Here, we report on the immobilisation of $[PMo_{12}O_{40}]^{3-}$ (POM) onto nano-SnO_2/FTO electrodes by electrostatic assembly with the polycation PDDA (polydiallyldimethylammonium chloride), using the LBL assembly approach. We demonstrate that by changing from planar FTO to nano-SnO_2/FTO electrodes the surface coverage of POM deposited in a single deposition step can be dramatically increased, removing the need for repeated dip-coat cycles. Significantly, the redox state of the films can be switched rapidly which is essential for many applications (i.e.: electrochromism). This method is broadly applicable, as shown by extending the method to polyoxotungstates and TiO_2 films, and could be used to rapidly immobilise moderate quantities of electroactive POM (tens of monolayers of material) in a single step.

2. Results and Discussion

2.1 Voltammetric properties: Figure 1 (a) shows the scan rate dependent cyclic voltammetry of a nano-SnO_2/FTO

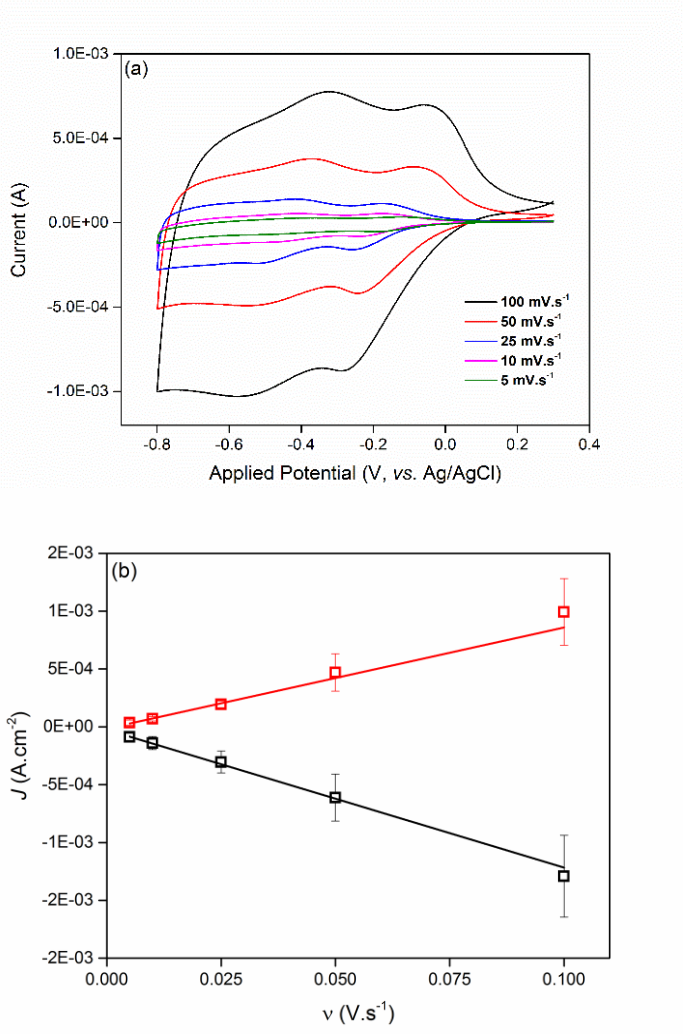

Fig. 1: (a) Scan rate dependent cyclic voltammetry of a nano-SnO_2/FTO film coated with PDDA-POM. (b) Plot of scan rate vs. peak current of the second redox process showing linear dependence. Slope data are averaged over two films, normalised for differences in area.

film coated with PDDA-POM where the supporting electrolyte is aqueous 0.1 M Na_2SO_4 (pH = 5.5). Redox features associated with $[PMo_{12}O_{40}]^{3-}$ are clearly present on the electrode surface with reductions at *ca*. -285 and -570 mV, and re-oxidations at -55 and -330 mV (CV vs. blank nano-SnO_2/FTO is shown in Fig. S1). These peaks are shifted to more negative potentials in comparison with those observed in solution (see Figs. S2, S3), a phenomenon which has

been seen with electrostatically immobilised POMs previously and attributed to electrostatic effects (ie: counterion exchange results in shifted POM redox potentials).[3, 10, 11] The solution resistance of a blank nano-SnO_2/FTO film was measured as 44 $\Omega.cm^{-2}$ at 0.2 V, and the adsorption of POM introduced a minor change in the overall resistance. Consistent with a surface confined response, the peak current increases linearly with increasing scan rate (Fig. 1 (b)); at scan rates greater than 1 $V.s^{-1}$, the large currents observed resulted in a significant iR drop. This behaviour makes it difficult to observe semi-infinite linear diffusion control where the depletion layer thickness is smaller than the film thickness. CVs of POM/PDDA adsorbed on planar FTO (Figs. S4, S5) showed the presence of the POM redox wave with E_{OX} = -335 mV and E_{RED} = 560 mV, however the reversibility of the wave is reduced on FTO; this kind of peak shifting has been observed previously for the immobilisation of POM films using $[P_2W_{17}O_{61}]^{10-}$ on planar conducting glass (ITO) electrodes.[10]

In the surface confined regime, the surface coverage, Γ, of electroactive material (i.e.: POM) can be calculated from the slope of the line and Equation 1:

$$i = \left(\frac{n^2F^2}{4RT}\right) vA\Gamma$$

where n is the number of electrons transferred, F is Faraday's constant (96485 $C.mol^{-1}$), R is the universal gas constant (8.314 $J.mol^{-1}.K^{-1}$), T is the temperature in Kelvin, and A is the geometric surface area in cm^2. Equation 1 yields POM Γ values of 8.7 x 10^{-10} $mol.cm^{-2}$ (Figs. S6, S7) for the planar FTO electrode and 1.5 ± 0.3 x 10^{-8} $mol.cm^{-2}$ for the nano-SnO_2/FTO electrode (with a typical nano-SnO_2 film thickness measured using a stylus profilometer to be *ca*. 2.1 µm, Fig. S8). These numbers are in-line with standard Γ values for single polyelectrolyte-POM bilayers on a planar surface (on the order of 5 x 10^{-10} $mol.cm^{-2}$)[12] and show that by using nano-SnO_2 as a support the surface coverage can be increased by a factor of approximately 17. Field emission scanning electron microscopy (FESEM) and Energy Dispersive X-ray (EDX) spectroscopic mapping showed molybdenum dispersed homogeneously across the sample (Figs. S9, S10).

2.2 Electrochromism: Electrochromism using immobilised POMs was originally reported using the LBL approach with polycations[13, 14] or cationic transition metal complexes;[15, 16] whereas more recent examples tend to focus on POM immobilisation on oxides such as TiO_2.[17, 18] The UV/Vis/NIR spectral response of the film was monitored as a function of potential. At +0.2 V the POM is fully oxidized and colourless. Stepping to -0.1 V generates a broad and featureless band stretching from 500 to 900 nm, attributed to the formation of the one electron reduced POM (Fig. S11). From -0.2 V, the maximum of the band resolved into a feature at 556 nm and grew-in with subsequent 100 mV potential steps to -0.8 V, accompanied by a blue shift to 510 nm. These changes in λ_{max} as a function of potential are non-linear and reflect the different redox states as observed by CV (Fig. S12), suggesting the stepwise formation of one, two and possibly three-electron reduced POM states.

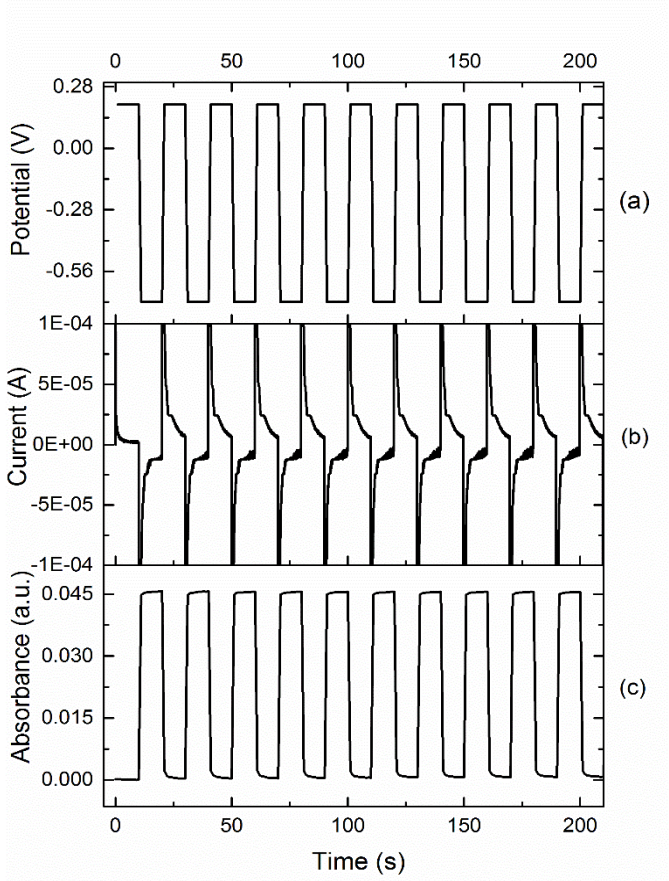

Fig. 2: Electrochromic response of a POM/PDDA film on nano-SnO_2/FTO. (a) Potential switching between + 0.2 V (oxidized) and -0.7 V (reduced) states. (b) Corresponding current passed as a function of potential switching. (c) Absorbance change at 700 nm as a function of potential switching.

As shown in Figure 2, the film could be switched between colourless and blue states by applying a modulating potential step sequence, and UV/Vis spectroscopy was used to measure the rates of colour change in the film. The switching of the film was fast, and > 90 % of the total absorbance change occurs in less than 1 second (1 s spectrometer resolution). The switching time is faster than, or comparable to, leading literature examples utilizing POM composite films,[19, 20] and this rapid switching is consistent with fast heterogeneous electron transfer across the POM/nano-SnO_2 interface. In addition, the switching response was stable, and over 25 cycles dropped by approximately 2 % (Fig. S13). In contrast, an unmodified nano-SnO_2/FTO film gave a very small optical response (Fig. S14), with a Δabs of < 5 % of that shown in Fig. 2. Fast, efficient electron transfer has been seen for similar systems previously; for example, photoinduced electron transfer has been observed in photoelectrodes of $[PMo_{12}O_{40}]^{3-}$ and SnO_2 nanowalls assembled by annealing rather than electrostatics, whereby the presence of immobilised $[PMo_{12}O_{40}]^{3-}$ resulted in increased photocurrent densities relative to SnO_2 alone.[21] The optical contrast (OC) of the film was calculated according to Equation 2:

$$OC = \frac{T_b - T_c}{T_b}$$

Where T_b and T_c are the transmittances of the bleached and coloured film, respectively, at the wavelength of max response. The coloration efficiency (CE) of the film, defined as the change in optical density per unit of charge consumed by the electrochromic layer is given by Equation 3:

$$CE = log\frac{T_b T_c}{q/A}$$

Where q is the charge passed (in Coulombs) and A is the geometric surface area of the electrode (in cm^2). Using Equations 2 and 3, the OC was calculated to be 11 % and CE calculated as 3.5 $cm^2.C^{-1}$; in contrast, typical literature values range from 20 to 200 $cm^2.C^{-1}$ for various POM based films (see also Table S1).[22, 23] While our device performance is modest, it is not the purpose of this study to report state of the art electrochromic efficiencies.

These data show the potential for fast electron transfer in POM/PDDA/nano-SnO_2/FTO films, which is highly promising for a wide range of applications. In addition, to demonstrate the generality of our approach, films of the corresponding polyoxotungstate $[PMo_{12}O_{40}]^{3-}$ were deposited onto nano-TiO_2/FTO electrodes using the same methodology (Figs. S15-S17). A Γ value of 1.3 ± 0.4 x 10^{-8} mol.cm^{-2} was measured, a factor of approximately 15 higher than on planar-FTO. These results clearly demonstrate the potential to expand this new methodology to hybrid POM/nanoparticle films of a wide range of compositions, including photoelectrochemistry.

3. Conclusions

SnO_2 nanoparticle films on FTO are an effective substrate for the deposition of the polyoxometalate $[PMo_{12}O_{40}]^{3-}$ by electrostatic adsorption with the polycation PDDA. By using nano-SnO_2 as the support, a 17x increase in POM surface loading was measured in comparison with a planar FTO slide. The POM/PDDA/nano-SnO_2/FTO films were measured to be on the order of 2.1 μm thick, with homogeneous dispersion of Mo across the film. The films exhibit fast electrochromic switching behaviour, good stability, and redox reversibility, suggesting that this method could be of use in other applications utilizing immobilised POMs such as catalysis and sensing. The benefits of this new method are fourfold. First, it is extremely simple, uses low-cost and commercially available materials, and results in materials that are optically transparent in the near-UV/visible/near infrared regions. Second, it is a much faster method to achieve POM surface coverages on the order of tens of monolayers than the alternating dip-coat LBL assembly usually reported. Third, it is a general approach and can be used to assemble either molybdates or tungstates onto a range of different substrates. Fourth, by coating what is effectively a high surface area electrode with a thin film, the POMs are always close to the electrode interface giving rise to efficient heterogeneous electron transfer (i.e.: fast bulk electrolysis of the film). This behaviour contrasts with that found for films comprised of $[Fe(bpy)_3]^{2+}$ and α/β-$[P_2W_{18}O_{62}]^{6-}$, used for electroanalytical sensing of nitrite,[24] where the surface coverages are similar to those achieved here but the films are not supported on a conducting nano support. By restricting the self-assembly process to a single dip-coat cycle, fast redox switching is assured. It also means that excessively high electrolyte concentrations can be avoided, which can disrupt the electrostatic interactions maintaining film integrity.[25] These excellent electrochemical characteristics could facilitate the use of POM/PDDA/MO_2 (M = Sn, Ti)/FTO films in a variety of applications including electrocatalytic sensing, photoelectrocatalysis, photoelectrochromic UV sensing, etc.

Acknowledgements

This publication has emanated from research conducted with the financial support of Science Foundation Ireland (SFI) under the Grant No. 15/SIRG/3517 (JJW). Funding for the FESEM was supported by SFI under Grant No. 03/IN.3/1361/EC07. We appreciate the contributions of Aisling McCarthy, (FESEM), Dr. Darragh Byrne and Prof. Enda McGlynn (TiO_2 film annealing and furnace access) as well as Prof. Robert J. Forster for laboratory facilities and on-going support of the programme.

Appendix A: Supplementary data available

References

1 Y.-F. Song and R. Tsunashima, *Chem. Soc. Rev*., 2012, **41**, 7384.
2 J. J. Walsh, A. M. Bond, R. J. Forster and T. E. Keyes, *Coord. Chem. Rev*., 2016, **306**, 217.
3 S. Imar, C. Maccato, C. Dickinson, F. Laffir, M. Vagin and T. McCormac, *Langmuir*, 2015, **31**, 2584.
4 J. Zhu, J. J. Walsh, A. M. Bond, T. E. Keyes and R. J. Forster, *Langmuir*, 2012, **28**, 13536.
5 P. Kang, S. Zhang, T. J. Meyer and M. Brookhart, *Angew. Chem. Int. Ed*., 2014, **53**, 1.
6 J. J. Walsh, J. Zhu, A. M. Bond, R. J. Forster and T. E. Keyes, *J. Electroanal. Chem*., 2013, **706**, 93.
7 M. Grätzel, *J. Photochem. Photobiol. C*, 2003, **4**, 145.
8 N. M. Muresan, J. Willkomm, D. Mersch, Y. Vaynzof and E. Reisner, *Angew. Chem. Int. Ed*., 2012, **51**, 12749.
9 P. G. Hoertz, Z. Chen, C. A. Kent and T. J. Meyer, *Inorg. Chem*., 2010, **49**, 8179.
10 S. Liu, L. Xu, G. Gao and B. Xu, *Thin Solid Films*, 2009, **517**, 4668.
11 L.-H. Bi, K. Foster, T. McCormac and E. Dempsey, *J. Electroanal. Chem*, 2007, **605**, 24.
12 Y. Wang, X. Wang, C. Hu and C. Shi, *J. Mater. Chem*., 2002, **12**, 703.
13 I. Moriguchi and J. H. Fendler, *Chem. Mater*., 1998, **10**, 2205.
14 D. Ingersoll, P. J. Kulesza and L. R. Faulkner, *J. Electrochem. Soc*., 1994, **141**, 140.
15 A. Kuhn and F. C. Anson, *Langmuir*, 1996, **12**, 5481.
16 G. Gao, L. Xu, W. Wang, W. An, Y. Qiu, Z. Wang and E.-B. Wang, *J. Phys. Chem. B*, 2005, **109**, 8948.
17 L. Liu, S.-M. Wang, C. Li, C.-G. Liu, C.-L. Ma and Z.-B. Han, *J. Mater. Chem. C*, 2015, **3**, 5175.
18 S.-M. Wang, L. Liu, W.-L. Chen, Z.-M. Zhang, Z.-M. Su and E.-B. Wang, *J. Mater. Chem. A*, 2013, **1**, 216.
19 D. Zhang, Y. Chen, H. Pang, Y. Yu and H. Ma, *Electrochim. Acta*, 2013, **105**, 560.

20 L. Liu, S.-M. Wang, C. Li, C.-G. Liu, C.-L. Ma and Z.-B. Han, *J. Mater. Chem. C*, 2015, **3**, 5175.
21 T. Wang, Z. Sun, F. Li and L. Xu, *Electrochem. Commun*., 2014, **47**, 45.
22 D. Zhang, Y. Chen, H. Pang, Y. Yu and H. Ma, *Electrochim. Acta*, 2013, **105**, 560.
23 B. Xu, L. Xu, G. Gao, W. Guo and S. Liu, *J. Colloid Interface Sci*., 2009, **330**, 408.
24 N. Fay, E. Dempsey and T. McCormac, *J. Electroanal. Chem*., 2005, **574**, 359.
25 J. J. Walsh, J. Zhu, Q. Zeng, R. J. Forster and T. E. Keyes, *Dalton Trans*., 2012, **41**, 9928.